Separation Science and Technology
Publication details, including instructions for authors and subscription information:
http://www.informaworld.com/smpp/title~content=t713708471

Effects of Thermal Treatment on Gas Transport Through Porous Silica Membranes

Tatsu Hirata[a]; Shuichi Sato[a]; Kazukiyo Nagai[a]
[a] Department of Industrial Chemistry, Meiji University, Tama-ku, Kawasaki, Japan

To cite this Article Hirata, Tatsu , Sato, Shuichi and Nagai, Kazukiyo(2005) 'Effects of Thermal Treatment on Gas Transport Through Porous Silica Membranes', Separation Science and Technology, 40: 14, 2819 — 2839
To link to this Article: DOI: 10.1080/01496390500333145
URL: http://dx.doi.org/10.1080/01496390500333145

Separation Science and Technology, 40: 2819–2839, 2005

ISSN 0149-6395 print/1520-5754 online
DOI: 10.1080/01496390500333145

Effects of Thermal Treatment on Gas Transport Through Porous Silica Membranes

Tatsu Hirata, Shuichi Sato, and Kazukiyo Nagai
Department of Industrial Chemistry, Meiji University, Tama-ku, Kawasaki, Japan

Abstract: The effects of thermal treatment from 180°C to 1150°C on the gas transport properties of porous silica membranes were systematically studied for various gases. The permeance of all gases, except for CO_2, has a maximum at 800°C. The CO_2 permeance was constant from 180°C to 600°C and then decreased monotonically. Membranes thermally treated at 1150°C did not exhibit any gas permeation because of pore collapse. The gas transport behavior follows a combination of Knudsen diffusion and surface diffusion for all gases tested except for carbon dioxide. The permeation of carbon dioxide is strongly affected by capillary condensation. We propose a new transport model composed of two components; that is, the Knudsen diffusion factor, α, and the surface diffusion factor, β. A transition was observed for α and β at around 800–900°C, which is close to the strain point of the membrane. This transition treatment temperature can be correlated with the changes in gas permeance. The model allows qualitative evaluation of gas transport through porous membranes regardless of their actual microporous structures.

Keywords: Gas transport, porous membranes, silica membranes, Knudsen diffusion, surface diffusion, capillary condensation, thermal treatment

Received 8 February 2005, Accepted 1 September 2005
Address correspondence to Kazukiyo Nagai, Department of Industrial Chemistry, Meiji University, 1-1-1 Higashi-mita, Tama-ku, Kawasaki 214-8571, Japan. Tel.: + 81-44-934-7211; Fax: +81-44-934-7906; E-mail: nagai@isc.meiji.ac.jp

INTRODUCTION

Gas transport through porous membranes with an average pore diameter of 10 Å–50 Å is affected by both Knudsen diffusion and surface diffusion. Capillary condensation can also occur for transport of condensable gases, such as carbon dioxide. A number of models for gas transport through porous membranes have been proposed by various groups (1–28). There are two types of studies. The one assumes that the pore structure was defined as an ideal tube-like structure in their gas transport theories (1, 2, 4–14, 16, 18–20, 23, 25–27). The other one is that the evaluated material was distorted and was completely different from the supposition (2, 3, 9, 15, 17, 21, 22, 24, 28). However, with the rapid development of visual analytical techniques, such as scanning electron microscopy (SEM), transmission electron microscopy (TEM), and atomic force microscopy (AFM), doubts have been raised about applying existing transport models. In many cases, photo images of porous membranes reveal quite different structures from those proposed in the models. For example, these models assumed that the pore structure was ideal tube-like. In this study, the effects of thermal treatment on gas transport in porous silica membranes were systematically investigated. We propose a simplified transport model that is valid for any porous membrane regardless of its actual microporous structure.

EXPERIMENTAL

Pretreatment of a Porous Silica Membrane

The physical properties of tubular porous silica membranes used in this study are summarized in Table 1 (29). The porous silica membrane studied was Vycor® glass 7930 (Corning Inc., New York, USA, outside diameter 10.5 mm, inner diameter 8.0 mm). This membrane can readily absorb organic compounds from the atmosphere. To remove these potential contaminants, the porous silica membranes were immersed into an aqueous 30 wt% hydrogen peroxide solution (Junsei Chemical Co., Ltd., Tokyo, Japan). After removing the membranes from the cleaning solution, they were thermally treated at 100°C for 10 min. The membranes were then washed several times with pure water, and afterward treated at 180°C under nitrogen for 1 h. These membranes were used as control membranes and were stored under vacuum prior to thermal treatment and permeation experiments.

Thermal Treatment of Control Porous Silica Membranes

Control membranes were thermally treated at 300, 500, 600, 700, 800, 900, 1000, and 1150°C. Because the silica membranes have a small thermal

Table 1. Physical properties of a porous silica membrane (corning code 7930)

Property	Value[a]
Outside diameter (mm)	10.5
Inner diameter (mm)	8.0
Composition	96% SiO_2, ~4% B_2O_3
Apparent density (g/cm^3)	1.45–1.50
Internal pore volume (%)	28
Internal surface area (m^2/g)	250
Average pore diameter (Å)	40
Water adsorption at saturation (wt%)	25
Strain point (°C)	890
Softening point (°C)	1530
Thermal expansion coefficient (°C)	7.5×10^{-7}

[a]Reference (29).

expansion coefficient of 7.5×10^{-7}°C, as noted in Table 1, a rapid thermal change easily produced cracks in the membranes in our preliminary experiments. Therefore, porous silica membranes were thermally treated using the following procedure. Control membranes were placed in an electric furnace (KDFs 70, Denken, Inc., Kyoto, Japan), and purged with nitrogen. The treatment temperature in the furnace was increased from room temperature to a given treatment temperature at a heating rate of 200°C/h. Thereafter, the treatment temperature was kept constant for 30 min and then it was decreased from 1150°C to 600°C at 550°C/h; from 600°C to 200°C and from 200°C to room temperature at 40°C/h. Thereafter, the shrinkage of thermally treated membranes was determined geometrically.

Gas Permeation Measurements

The gas permeance of thermally treated porous silica membranes was determined by a constant volume-variable pressure method at 35°C. The gases employed in this study were hydrogen (H_2), helium (He), methane (CH_4), nitrogen (N_2), ethane (C_2H_6), oxygen (O_2), carbon dioxide (CO_2), and propane (C_3H_8). The physical properties of these gases are summarized in Table 2 (30–32). The upstream pressure was 20 cmHg, whereas the downstream pressure was maintained under vacuum. The permeance, Q [in GPU $= 10^{-6}\,cm^3(STP)/(cm^2 s\,cmHg) = 3.347 \times 10^{-10}\,mol/(m^2\,s\,Pa)$] was determined from Eq. (1)

$$Q = \frac{dp}{dt}\frac{273V}{760(273+T)}\frac{1}{S_a}\frac{1}{p_1} \tag{1}$$

Table 2. Physical properties of gases

Gas	M[a] (g/mol)	Kinetic diameter[b] (Å)	V_c [a] (cm^3/mol)	T_c [a] (K)	ρ_c [c] × 10^3 (g/cm^3)
H_2	2.02	2.89	65.0	33.3	31.6
He	4.00	2.60	57.3	5.19	69.6
CH_4	16.0	3.80	98.6	191	162
N_2	28.0	3.64	90.1	126	314
C_2H_6	30.1	4.00	146	305	205
O_2	32.0	3.46	73.4	155	436
CO_2	44.0	3.30	94.1	304	4661
C_3H_8	44.1	4.30	200	370	217

[a]Reference (30).
[b]Reference (31).
[c]Reference (32).

where dp/dt is the pressure increase in time at steady-state, V (cm^3) is the downstream volume, T (K) is the temperature, Sa (cm^2) is the membrane area, and p_1 (cmHg) is the upstream pressure. The feed gas permeated from the outside to the lumen of the tubular porous silica membranes. The experiments were performed for at least three samples to confirm the reproducibility of the results. The experimental uncertainty was less than 2% so that each error bar was masked in the size of symbols in all figures in this study.

Pore and Surface Structure Analysis

The pore size and its distribution in the porous silica membranes were determined at 35°C using a Nano–Perme Porometer (Model: TNF3WH110MSE, Seika Co., Tokyo, Japan). The surface structure of porous silica membranes was analyzed by AFM (Nanoscope multi-mode, Veeco Inc, Santa Barbara, USA), at a tapping mode using a single crystal silicone probe. The AFM images were displayed with resolutions of 512–256 nm.

RESULTS AND DISCUSSION

Porous Structures

Shelekhin et al. reported on the shrinkage of Vycor®-type porous silica membranes (no information on the product code) (33). The shrinkage ratio as a function of thermal treatment temperature is displayed in Fig. 1. Our experimental results are consistent with those obtained by Shelekhin et al.;

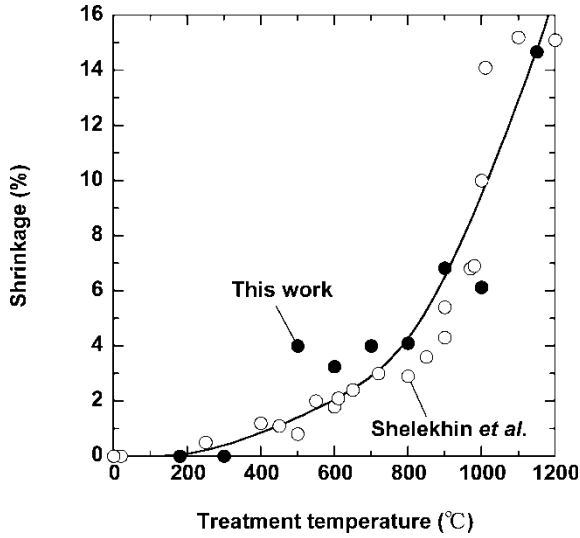

Figure 1. Dependence of the shrinkage of Vycor®-type porous silica membranes on the treatment temperature. This work (●); Shelekhin et al. (33) (○).

that is, shrinkage increases approximately exponentially as the treatment temperature increases. At 1150°C, the highest treatment temperature in this study, the shrinkage was about 15%. In previous studies, boric acid was liberated from the membrane surface from 600 to 900°C (34–39). Decomposition and/or crosslinking of siloxane bonds and silanol groups might have occurred by heat treatment at >1000°C. This could explain the shrinkage behavior shown in Fig. 1.

AFM images of the surfaces of the porous silica membranes thermally treated at 180°C (i.e., control membranes), 1000°C, and 1150°C are shown in Fig. 2. The shrinkage percentage was 0% at 180°C, 6.13% at 1000°C, and 14.7% at 1150°C, as shown in Fig. 1. The surface structure around a pore of thermally treated membranes at 180°C shows a heterogeneous pore size with a structure formed by assembled nano-silica particles.

As the treatment temperature increases, nano-silica particles tend to melt and the surface becomes smooth. Fig. 3 presents the average surface roughness of the AFM images in Fig. 2 as a function of treatment temperature. The average roughness is about 5 nm and is constant from 180°C to 1000°C, as expected from the AFM images in Fig. 2. The roughness at 1150°C had the largest value of 22 nm. As shown in Fig. 2, the surface of membranes heated to 1150°C became smooth, indicating melt sintering of the particles. This result indicates that a distinct structural change occurred between 1000°C and 1150°C. As discussed next, gases did not permeate through membranes thermally treated at 1150°C.

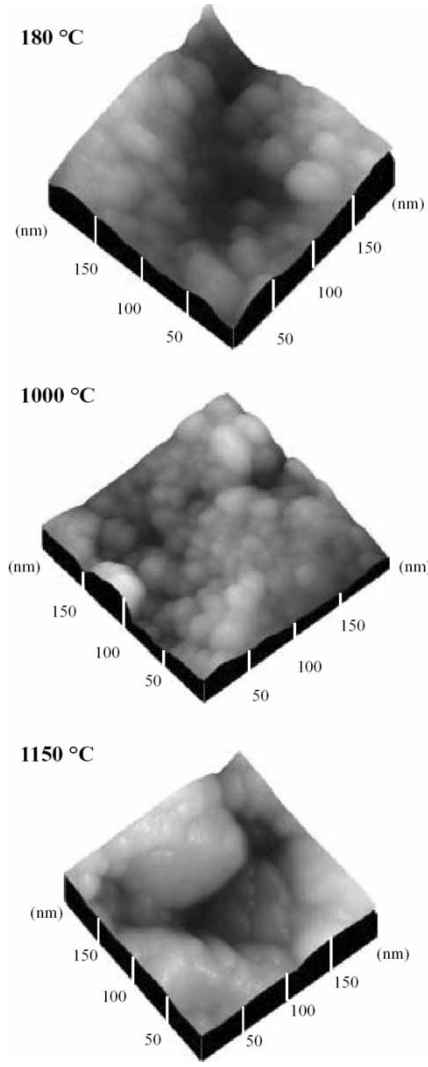

Figure 2. AFM images of the surface of the porous silica membranes thermally treated at 180°C (control), 1000°C, and 1150°C.

Fig. 4 presents the pore size distribution in the porous silica membranes thermally treated at 180°C, 800°C, and 900°C. The pore size distribution of all membranes varies from 0.5 nm to 5.0 nm. The average pore diameter is 26 Å for membranes treated at 180°C and 23 Å for those treated at 800 and 900°C. The strain point of porous silica membranes is 890°C, as noted in Table 1 (29). On the basis of the results presented in Fig. 3, the pore size is slightly reduced around this treatment temperature by assembling

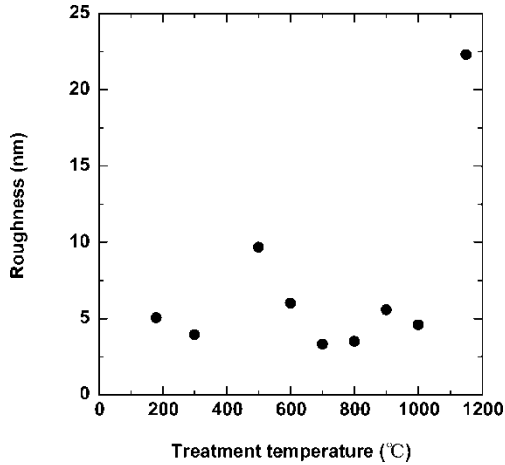

Figure 3. Dependence of the surface roughness of the porous silica membranes on treatment temperature.

(or shrinking) of nano-particles, which leads to an increase in the surface density.

Gas Transport

There are abundant experimental data in the literature regarding gas permeance or permeability through porous Vycor® glass. For example,

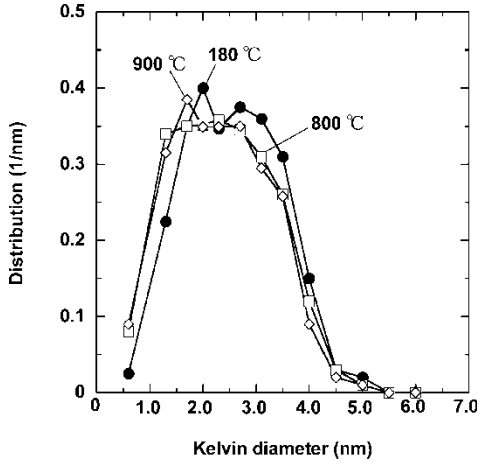

Figure 4. Pore size distribution in the porous silica membranes thermally treated at 180°C (●), 800°C (□), and 900°C (◇).

there are more than 50 publications by the literature search result of SciFinder®. Previously, several studies reported the gas permeation properties of tubular-type Vycor® membranes (2, 10, 22, 28, 33, 40). The permeability of Vycor glass is strongly influenced by the pretreatment and/or preservation methods. Among various publications, the gas transport experiments in only (2) and (22) were performed at the same conditions of ours. Hence, we compared our data with those in only (2) and (22). Table 3 summarizes the permeance at 35°C of our control membrane (i.e., thermally-treated at 180°C) with some data from the literature. The permeance varies from 180 GPU for H_2 to 51 GPU for O_2. The data of our control membrane for H_2, He, CH_4, N_2, O_2, and CO_2 are in good agreement with the data reported by Hwang and Kammermeyer and Fernandes and Gavalas (2, 22).

The gas permeances for the non-condensable gases (i.e., H_2, He, N_2, and O_2) at 35°C in the porous silica membrane thermally treated from 180°C to 1150°C are shown in Fig. 5a. Figure 5b presents the gas permeance at 35°C of the same membranes to condensable gases (i.e., C_2H_6, CO_2 and C_3H_8) and to a permanent gas (CH_4). Regardless of the treatment temperature, except for 1150°C, the ranking of the gas permeance is $H_2 > He > C_3H_8 > CH_4 > C_2H_6 > CO_2 > N_2 > O_2$. Membranes thermally treated at 1150°C did not show any measurable gas permeation, indicating collapse of the pores.

To elucidate the effects of thermal treatment, changes in permeance as a function of treatment temperature can be described by

$$\frac{Q_{T^\circ C}}{Q_{180^\circ C}} \tag{2}$$

where $Q_{T^\circ C}$ is the permeance for membranes treated at a specific temperature and $Q_{180^\circ C}$ is the permeance of the control membrane. The $Q_{T^\circ C}/Q_{180^\circ C}$ values as a function of the treatment temperature for non-condensable gases and condensable gases are shown in Fig. 6a and 6b. The permeance ratio of non-condensable gases decreases slightly with increasing treatment temperature up to 600°C and then increases up to 800°C. At higher treatment temperature

Table 3. Gas permeance at 35°C through control membranes

	Permeance (GPU)							
Author	H_2	He	CH_4	N_2	C_2H_6	O_2	CO_2	C_3H_8
Hirata et al.	180	130	76	54	72	51	68	79
S.T. Hwang and K. Kammermeyer[a]	193	136	—	57	—	53	65	—
Fernandes and Gavalas[b]	181	—	72	55	—	—	—	—

[a]These values at 35°C were estimated from the figures in reference (2).
[b]These values at 35°C were estimated from the figures in reference (22).

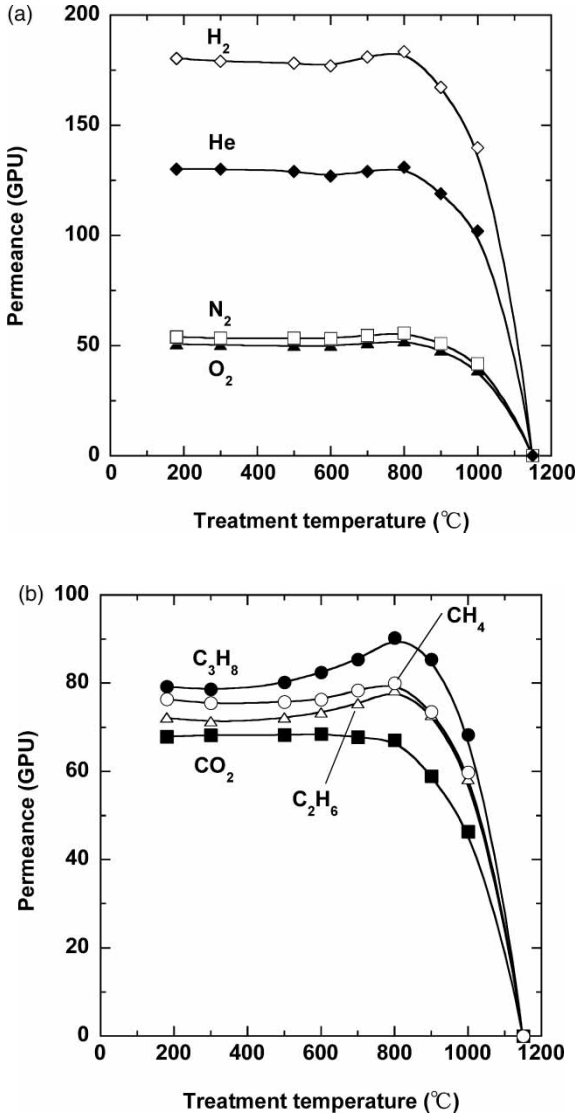

Figure 5. Permeance at 35°C of (a) non-condesable gases and (b) condensable gases through porous silica membranes as a function of treatment temperature. Gases; hydrogen (◇), helium (◆), methane (○), nitrogen (□), ethane (△), oxygen (▲), carbon dioxide (■), and propane (●).

it decreased significantly for all gases except for CO_2. The ratio of CO_2 does not show a maximum at 800°C but rather decreases monotonically above 600°C. In fact, this reason was not clear. According to Rhim and Hwang, this behavior is explained as capillary condensation (9). They proposed six

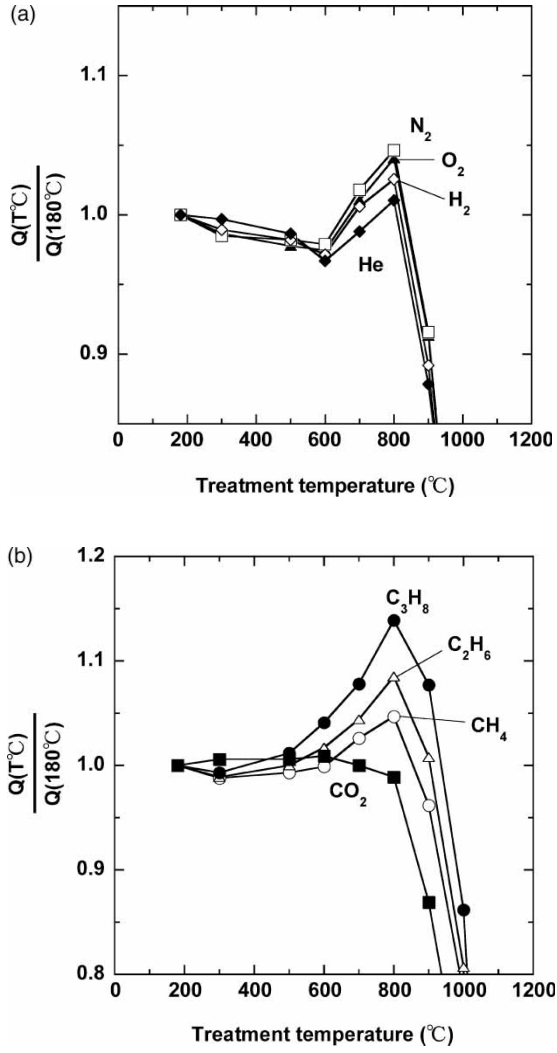

Figure 6. Permeance ratio, Q (T°C)/Q (180°C), at 35°C of thermally treated porous silica membranes for (a) non-condensable gases and (b) condensable gases. Gases: hydrogen (◇), helium (◆), methane (○), nitrogen (□), ethane (△), oxygen (▲), carbon dioxide (■), and propane (●). Q (180°C): gas permeance at 35°C of membranes thermally treated at 180°C (control membranes). Q (T°C): gas permeance at 35°C of membranes thermally-treated at 300, 500, 600, 700, 800, 900, 1000, and 1150°C.

flow models for capillary condensation from Eq. (10). In this study, among the gases tested, only the CO_2 transport was good agreement with the six flow models (i.e., F_2 model). This is probably because the density of condensate, ρ_c of CO_2 is much higher than the other gases, as noted in Table 2. To

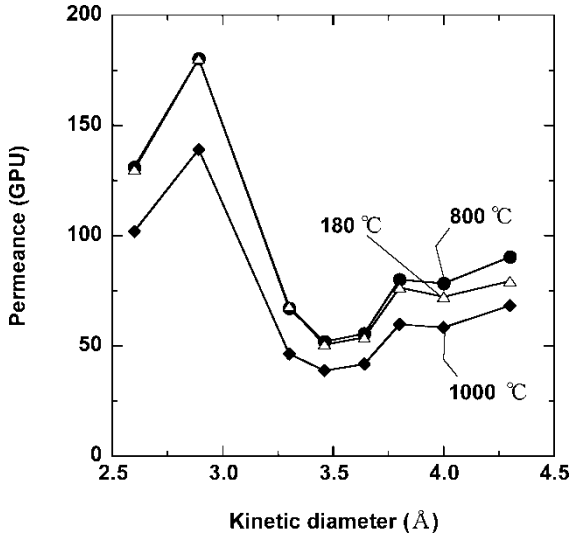

Figure 7. Permeance at 35°C of various gases through porous silica membranes as a function of the gas kinetic diameter. Treatment temperatures: 180°C (△), 800°C (●), and 1000°C (◆).

understand this phenomenon, the further research is necessary. In this article, we have used the date except for carbon dioxide for the analysis of the transport.

The gas permeance of porous membranes is often presented as a function of the penetrant kinetic diameter to elucidate their size sieving ability. Fig. 7 presents the gas permeance at 35°C of porous silica membranes thermally treated at 800°C (i.e., maximum permeance ratios in Fig. 6) and 1000°C (i.e., lowest permeance ratios in Fig. 6a and 6b) with the control membrane (i.e., thermally-pretreated at 180°C). The permeance for all gases tested can not simply be correlated with the gas molecular size. This result indicates that, regardless of the treatment temperature, the gas transport of silica membranes does not follow the size sieving effect typically observed in other porous membranes.

Gas Transport Model

The gas permeance, Q, through a porous membrane can be described as the sum of Q_g, the Knudsen diffusion contribution, and Q_s, the surface diffusion contribution (10, 13):

$$Q = Q_g + Q_s \tag{3}$$

Q_g is given by

$$Q_g = \frac{SG_1}{\sqrt{2\pi MRT}} \tag{4}$$

where S (cm^2) is the macroscopic cross-sectional area of a microporous medium, G_1 is a geometric factor correlated to porosity and tortuosity, M (g/mol) is the molecular weight of the gas, R (erg/(K g mol)) is the gas constant, and T (K) is the temperature. The Knudsen diffusion gas permeance, Q_g, is independent of gas pressure.

Q_s can be expressed as

$$Q_s = \frac{F_s L}{S\Delta p} = \frac{RT\rho_{app}}{C_R S\tau^2}\frac{x^2}{p} \tag{5}$$

where F_s is the flow rate, Δp (cmHg) is the pressure difference, x is the amount adsorbed (g mol/g) L (cm) is the thickness of the porous medium, ρ_{app} (g/cm^3) is the apparent density of a porous material, C_R is the resistance coefficient, and τ is the tortuosity.

Eq. (3) can be transformed to Eq. (6) (2, 3, 10).

$$Q\sqrt{MT} = A + BTe^{\Delta/T} = A + a(V_c\sqrt{T_c})^b \tag{6}$$

where A (cm^3(STP)$K^{0.5}$/(cm^2 s cmHg mol)) is the Knudsen diffusion constant, B (g mol/(cm^3 $K^{0.5}$)) is the surface diffusion coefficient, and Δ (K) is the interaction factor of gas molecules. These three parameters are defined as

$$A = \frac{G_1}{\sqrt{2\pi R}} \tag{7}$$

$$\Delta = \frac{\varepsilon_1 - \varepsilon_2}{k} \tag{8}$$

$$B = \frac{G_2}{\sqrt{2\pi R}}\frac{k}{2\pi M\nu_y\nu_z} \tag{9}$$

where G_1 is a geometric factor related to the pore size, porosity, and tortuosity, G_2 is a geometric factor related to the density and porosity, M (g/mol) is the molecular mass of a molecule, ε_1 is the minimum potential energy for an adsorbed molecule, ε_2 is the activation energy of surface diffusion for an adsorbed molecule, k is the Boltzmann constant ($=1.38 \times 10^{-10}$ erg/K), ν_y is the frequency of a harmonic oscillator in y-directional motion, and ν_z is the frequency of a harmonic oscillator in z-directional motion.

The capillary condensation pressure, p_l, can be estimated by the Kelvin equation (13, 20)

$$\frac{\rho_c RT}{M}\ln\frac{p_l}{p_0} = -\frac{2\sigma\cos\theta}{r} \tag{10}$$

where p_0 (cmHg) is the saturated vapor pressure for a planar interface, ρ_c (g/cm^3) is the density of the condensate, σ (dyn/cm) is the interfacial tension, θ is the contact angle, and r (cm) is the radius of a cylindrical capillary. The contact angle between a porous silica membrane and each gas is approximately zero.

The gas permeation data in Fig. 5 are analyzed using an existing transport model based on Eq. (6). Because G_1 in Eq. (7) is unknown, the three adjustable parameters (i.e, A, Δ, and B) were simply determined from curve fitting in Fig. 5.

The A value (i.e., Knudsen diffusion coefficient) and Δ and B values (i.e, surface diffusion coefficients) are plotted as a function of treatment temperature in Figs. 8–10, respectively. In Fig. 8, the A value is constant from 180°C to 800°C. However, at higher treatment temperatures, the A value dropped significantly. For membranes treated at 1150°C the A value becomes zero because gas permeation through the membranes decreased to zero. As shown in Fig. 6, the gas permeance exhibited the same treatment temperature dependence behavior. This result indicates that Knudsen diffusion contributes to the total gas transport through the silica membranes.

As the treatment temperature increased up to 1000°C, the Δ value increased exponentially, as shown in Fig. 9. On the other hand, the B value decreases exponentially, as shown in Fig. 10. The Δ and B values were zero at 1150°C, because there was no measurable gas permeation through the membranes. An increase in Δ is probably due to an increase in minimum potential energy for an adsorbed molecule, ε_1 and/or a decrease in the

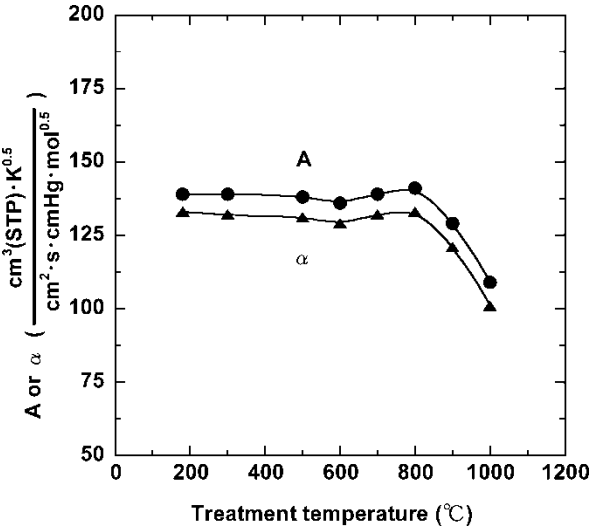

Figure 8. Parameter A in Eq. (6) and parameter α in Eq. (11) as a function of treatment temperature.

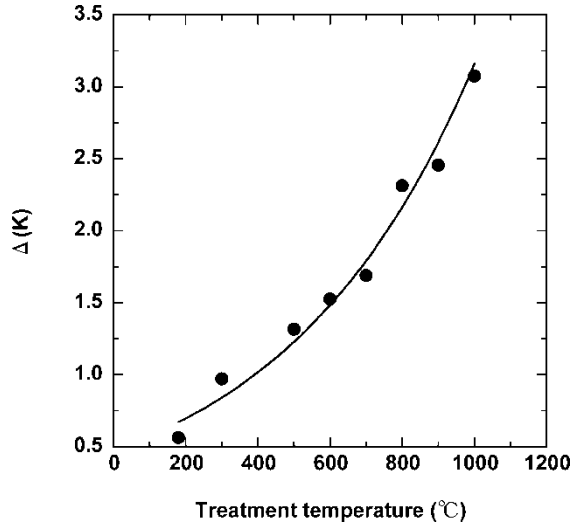

Figure 9. Parameter Δ of porous silica membranes as a function of treatment temperature.

activation energy of surface diffusion for an adsorbed molecule, based on Eq. (8). A decrease in the B value would result from an increase in the frequency of a harmonic oscillator in the y-directional motion, ν_y and in the z-directional motion ν_z.

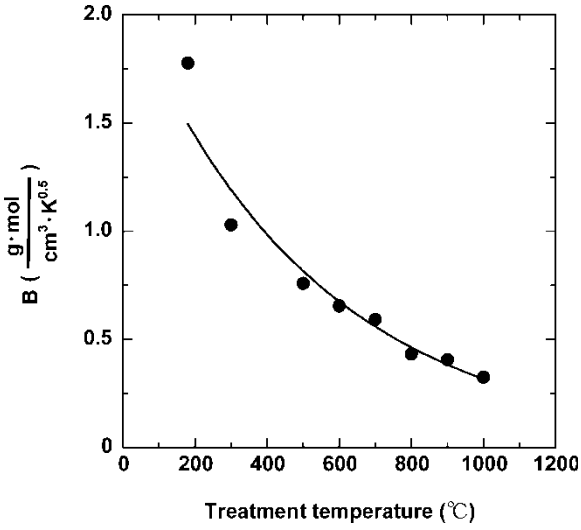

Figure 10. Parameter B of porous silica membranes as a function of treatment temperature.

For the Δ and B values, no transition was observed in contrast to the A value. This result suggests that Knudsen diffusion dominates gas transport through these porous silica membranes.

In this study, we propose a new transport model, that is, Eq. (11), composed of only two simplified parameters α ($cm^3(STP)K^{0.5}/(cm^2\,s\,cmHg\,mol)$) and β ($g\,mol/(cm^3\,K^{0.5})$), which are independent of *real* geometric pore structures

$$Q\sqrt{MT} = \alpha e^{\beta(V_c\sqrt{T_c})} \tag{11}$$

where α is the Knudsen diffusion factor and β is the surface diffusion factor. These two parameters can be used for the relative evaluation of gas transport in porous membranes.

Both Eqs. 6 and 11 contributed to surface diffusion and Knudsen diffusion. The parameters in Eq. (6) with three parameters were values for the absolute comparison between surface diffusion and Knudsen diffusion. The other hands, the two parameters in Eq. (11) were values for the relative comparison between surface diffusion and Knudsen diffusion. Therefore, Eq. (11) was not simply equal to Eq. (6). As previously described, Eq. (11) was also proposed to evaluate distorted materials. Fig. 11 presents $Q(MT)^{0.5}$ for the control membrane as a function of $V_c(T_c)^{0.5}$. The α is the intercept of the straight line and is related to the pore size, tortuosity, and porosity for Knudsen diffusion. The values of porosity and tortuosity are not

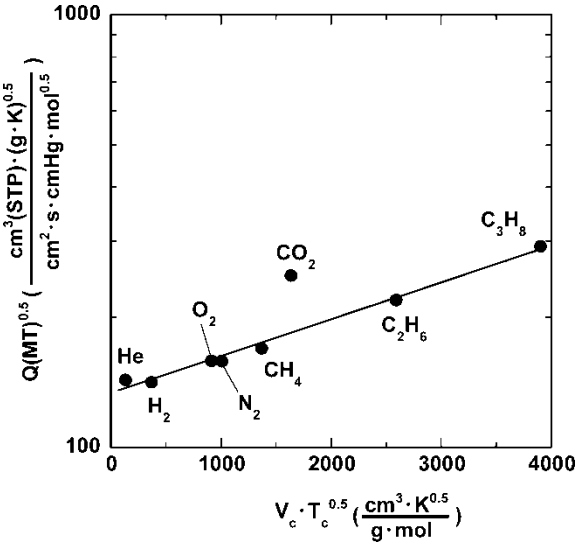

Figure 11. $Q(MT)^{0.5}$ as a function of $V_c(T_c)^{0.5}$ for porous silica membranes thermally-treated at 180°C. The line represents the best fit to the data except for carbon dioxide. The permeance data are from Fig. 5.

necessary to determine α. The β value is determined from the slope of the line and is related to the apparent surface density of the membrane for surface diffusion. Like α, the surface density value is not required to determine β. We have assumed that α is equal to the Knudsen diffusion coefficient A in Eq. (6), and β is related to both the surface diffusion coefficient B and the interaction factor Δ. The contribution of the surface diffusion decreases, as a gas molecule becomes smaller. Hence, the contribution of the Knudsen diffusion increases in the total transport. When $V_c \to 0$ and $T_c \to 0$, the contribution of the surface diffusion is minimized; that is, $Q(MT)^{0.5} = A$ in Eq. (6), and $Q(MT)^{0.5} = \alpha$ in Eq. (11) Therefore α is equal to A. The α values are plotted in Fig. 8 with the A values. The α should be equal to the A with the same units. The A values are, however, a little bit higher than the α values for treatment temperatures up to 1000°C. This variation is probably due to the curve fitting uncertainties with multiple parameters. As is evident from this figure, both α and A show the same temperature dependence behavior. The α and A values are constant from 180°C to 800°C. Furthermore, as the treatment temperature increases, the α and A values decrease significantly. Both values are zero at 1150°C because there was no measurable gas permeation through the membranes at this treatment temperature. In Fig. 6, the gas permeance showed the same treatment temperature dependence behavior. Because α is a Knudsen diffusion factor and even if the geometric structures of the membranes change, it does not influence the permeance from 180°C to 800°C.

Figures 12 and 13 present the β value of the control membrane as a function of the parameters Δ and B, respectively. The $\beta \cdot V_c \cdot T_c^{0.5}$ values

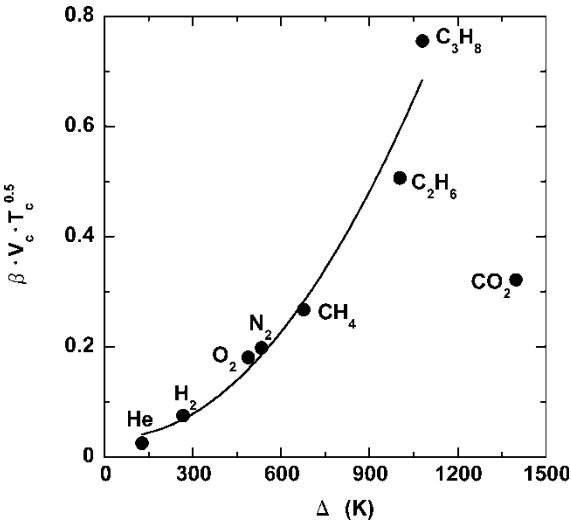

Figure 12. $\beta \cdot V_c \cdot T_c^{0.5}$ of porous silica membranes as a function of Δ.

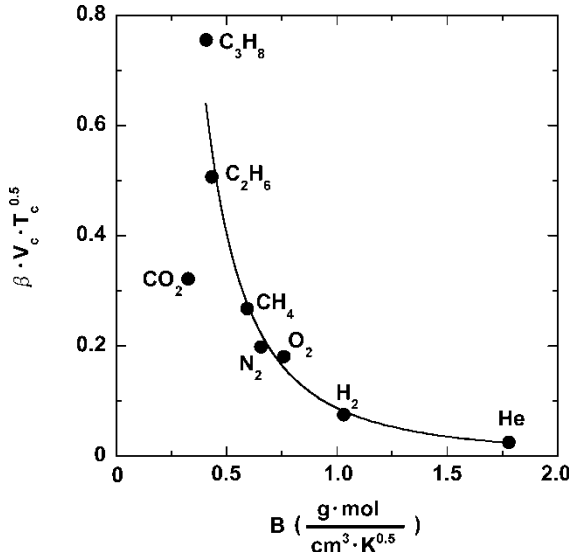

Figure 13. $\beta \cdot V_c \cdot T_c^{0.5}$ of porous silica membranes as a function of B.

increase exponentially with increasing Δ values. On the other hand, it decreases exponentially with increasing B values, for all gases except carbon dioxide. The β correlates to both Δ and B. Therefore, we assume the parameter β relates to surface diffusion. The same trend appears for other silica membranes thermally treated between 300°C and 1000°C.

Figure 14 presents β values as a function of treatment temperature. As the treatment temperature increases to 900°C, the β value increases exponentially and then decreases quickly with increasing treatment temperature. The β value is zero at 1150°C. This indicates that the effect of surface diffusion on transport increases with increasing treatment temperature up to 900°C. The AFM images in Fig. 2 indicated that the unevenness surface structure became smoother with increasing treatment temperature. The change of the surface smoothness probably caused an increase in β. The inside pores would be shrank and blocked significantly from 900°C. Therefore, β decreased quickly with increasing treatment temperature from 900°C.

Hence, Knudsen diffusion and surface diffusion can occur simultaneously. Based on Fig. 6, surface diffusion probably contributes more to the total transport for membranes treated at 800°C compared to Knudsen diffusion.

Based on the analysis provided by Eq. (11), a transition was observed for the α and β values around 800–900°C, which is close to the strain point. This transition treatment temperature can be correlated to changes in the gas permeance, as shown in Fig. 5. In this regard, Eq. (11) is effective to

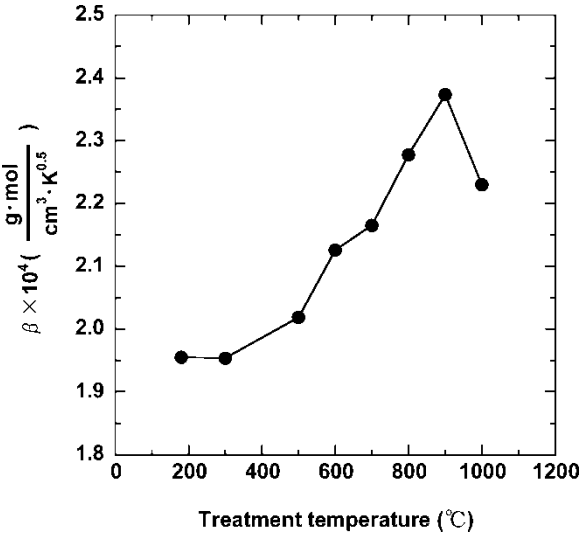

Figure 14. Parameter β of porous silica membranes as a function of treatment temperature.

evaluate the treatment temperature dependence on gas transport in porous membranes, regardless of their exact geometric properties, such as the pore size, tortuosity, and porosity.

CONCLUSIONS

The effects of thermal treatment from 180°C to 1150°C on gas transport properties of porous silica membranes were systematically studied for hydrogen, helium, methane, nitrogen, ethane, oxygen, carbon dioxide, and propane. The permeance of non-condensable gases decreases slightly with increasing treatment temperature up to 600°C and then increases up to 800°C. Thereafter, the permeance decreases significantly. The same trend is observed for condensable gases, except for CO_2. The permeation ratio of CO_2 does not show a maximum at 800°C and instead decreases regularly above 600°C. Membranes thermally treated at 1150°C did not show any gas permeation because of pore collapse. Gas transport behavior in the silica membranes follows a combination of Knudsen diffusion and surface diffusion for all gases tested, except for carbon dioxide. The carbon dioxide transport is strongly affected by capillary condensation. We have proposed a new transport model in Eq. (11) composed of two factors; that is, the Knudsen diffusion factor, α, and the surface diffusion factor, β. A transition was observed for α and β at around 800–900°C, which is close to the strain

point of the membrane. This transition treatment temperature can be correlated with the observed change in the gas permeance. The model allows the relative evaluation of gas transport properties of porous membranes regardless of their actual microporous structures.

ACKNOWLEDGMENT

The authors would like to thank Ms. Masami Saito at Veeco Inc., Tokyo, Japan for providing the images of the surface structure analysis by AFM and Mr. Yaza Takehiko at Seika Co., Tokyo, Japan for providing the pore size distribution analysis by a Nano-Perm Porometer.

REFERENCES

1. Knudsen, M. (1952) The kintetic theory of gases-some modern aspects. In *Methuens Monografhs on Physical Subjects*; London, 1–61.
2. Hwang, S.T. and Kammermeyer, K. (1966) Surface diffusion in microporous media. *Can. J. Chem. Eng.*, 44: 82–89.
3. Hwang, S.T. (1968) Interaction energy in surface diffusion. *AIChE J.*, 14: 809–811.
4. Studt, P.L., Shackelford, J.F., and Fulrath, R.M. (1970) Solubility of gases in glass—a monatomic model. *J. Appl. Phys.*, 41 (7): 2777–2780.
5. Horiguchi, Y., Hudgins, R.R., and Silveston, P.L. (1971) Effect of surface heterogeneity on surface diffusion in microporous solids. *Can. J. Chem. Eng.*, 49: 76–87.
6. Masaryk, J.S. and Fulrath, R.M. (1972) Diffusivity of helium in fused silica. *J. Chem. Phys.*, 59 (3): 1198–1202.
7. Shackelford, J.F., Studt, P.L., and Fulrath, R.M. (1972) Solubility of gases in glass. II. He, Ne, and H_2 in fused silica. *J. Appl. Phys.*, 43 (4): 1619–1626.
8. Gilliland, E.R., Baddour, R.F., Perkinson, G.P., and Sladek, K.J. (1974) Diffusion on surfaces. I. Effect of concentration on the diffusivity of physically adsorbed gases. *Ind. Eng. Chem. Fundam.*, 13: 95–99.
9. Rhim, H. and Hwang, S.T. (1975) Transport of capillary condensate. *J. Colloid. Interface Sci.*, 52: 174–181.
10. Hwang, S.T. (1976) Surface diffusion parallel with Kunudsen flow. *Sep. Sci.*, 11: 17–27.
11. Okazaki, M., Tamon, H., and Toei, R. (1981) Interpretation of surface flow phenomenon of adsorbed gases by hopping model. *AIChE J.*, 27: 262–270.
12. Altena, F.W., Knoef, H.A.M., Heskamp, H., Bargeman, D., and Smolders, C.A. (1983) Some comments on the applicability of gas permeation methods to characterize porous membranes based on improved experimental accuracy and data handling. *J. Membrane Sci.*, 12: 313–322.
13. Lee, K.H. and Hwang, S.T. (1986) The transport of condensible vapors through a microporous vycor glass membrane. *J. Colloid. Interface Sci.*, 110: 544–555.
14. Krishna, R. (1987) A simplified procedure for the solution of the Dusty gas model equations for steady-state transport in non-reacting systems. *Chem. Eng. J.*, 35: 75–81.

15. Uhlhorn, R.J.R., Keizer, K., and Burggraaf, A.J. (1989) Gas and surface diffusion in modified γ-alumina systems. *J. Membrane Sci.*, 46: 225–241.
16. Schofield, R.W., Fane, A.G., and Fell, C.J.D. (1990) Gas and vapor transport through microporous membranes. I. Knudsen-poiseuille transition. *J. Membrane Sci.*, 53: 159–171.
17. Keizer, K., Uhlhorn, R.J.R., Zaspalis, V.T., and Burggraaf, A.J. (1991) Transport and related (Gas and vapour) separation in ceramic membranes. *Key Eng. Mater.*, 61&62: 143–154.
18. Xiao, J. and Wei, J. (1992) Diffusion mechanism of hydrocarbons in zeolites. I. *Theory. Chem. Eng. Sci.*, 47 (5): 1123–1141.
19. Datta, R., Dechapanichkul, S., Kim, J.S., Fang, L.Y., and Uehara, H. (1992) A generalized model for the transport of gases in porous, non-porous, and leaky membranes. I. Application to single gases. *J. Membrane Sci.*, 75: 245–263.
20. Bhandarkar, M., Shelekhin, A.B., Dixon, A.G., and Ma, Y.H. (1992) Adsorption, permeation, and diffusion of gases in microporous membranes. I. Adsorption of gases on microporous glass membranes. *J. Membrane Sci.*, 75: 221–231.
21. de Lange, R.S.A., Keizer, K., and Burggraaf, A.J. (1995) Analysis and theory of gas transport in microporous sol-gel derived ceramic membranes. *J. Membrane Sci.*, 104: 81–100.
22. Fernandes, N.E. and Gavalas, G.R. (1997) Gas transport in porous vycor glass subjected to gradual pore narrowing. *Chem. Eng. Sci.*, 53: 1049–1058.
23. Meixner, D.L. and Dyer, P.N. (1998) Characterization of the transport properties of microporous inorganic membranes. *J. Membrane Sci.*, 140: 81–95.
24. Burggraaf, A.J. (1999) Single gas permeation of thin zeolite (MFI) membranes: theory and analysis of experimental observations. *J. Membrane Sci.*, 155: 45–65.
25. Sidhu, P.S. and Cussler, E.L. (2001) Diffusion and capillary flow in track-etched membranes. *J. Membrane Sci.*, 182: 91–101.
26. Wood, J. and Gladden, L.F. (2002) Modelling diffusion and reaction accompanied by capillary condensation using three-dimensional pore networks. Part 1. Fickian diffusion and pseudo-first-order reaction kinetics. *Chem. Eng. Sci.*, 57: 3033–3045.
27. Schoen, M. (2002) Capillary condensation between mesocopically rough surfaces. Colloids and Surfaces A. *Physicochem. Eng. Aspects.*, 206: 253–266.
28. Lee, D. and Oyama, S.T. (2002) Gas permeation characteristics of a hydrogen selective supported silica membrane. *J. Membrane Sci.*, 210: 291–306.
29. Yamane, M., Yasui, I., Wada, M., Kokubu, Y., Terai, R., Kondo, K., and Ogawa, S. (1999) Garasukougaku handbook, 480.
30. Poling, B.E. (2001) *The Properties of Gases and Liquids*; McGraw-Hill.
31. Barsema, J.N., van der Vegt, N.F.A., Koops, G.H., and Wessling, M. (2002) Carbon molecular sieve membranes prepared from porous fiber precursor. *J. Membrane Sci.*, 205 (1–2): 239–246.
32. Murata, S. (2004) Kagakubinnrann basic II, 130–133.
33. Shelekhin, A.B., Pien, S., and Ma, Y.H. (1995) Permeability, surface area, pore volume and pore size of Vycor glass membrane heat-treated at high temperatures. *J. Membrane Sci.*, 103: 39–43.
34. Dawidowicz, A.L., Nazimek, D., Pikus, S., and Skubiszewska, J. (1984) The influence of boron atoms on the surface of controlled porous glasses on the properties of the carbon deposit obtained by pyrolysis of alcohol. *J. Anal. Appl. Pyrolysis*, 7: 53–63.
35. Dawidowicz, A.L. (1986) Study of surface of the thermally treated porous glasses used as supports of chemically bonded phases. *Chem. Anal.*, 31: 385–395.

36. Dawidowicz, A.L. and Pikus, S. (1987) The influence of long additional thermal treatment of controlled porous glasses on the structuralization of their silica network. *J. Thermal Analysis*, 32: 409–415.
37. Wang, D.S. and Pantano, C.G. (1992) Surface chemistry of multicomponent silicate gels. *J. Non-Cryst Solids*, 147 & 148: 115–122.
38. Carteret, C. and Burneau, A. (2000) Effect of heat treatment on boron impurity in vycor. I. Near infrared spectra and ab initio calculations of the vibrations of model molecules for surface boranols. *Phys. Chem. Chem. Phys.*, 2: 1747–1755.
39. Carteret, C. and Burneau, A. (2000) Effect of heat treatment on boron impurity in vycor. II. Migration, reactivity with vapour water and dissolution in liquid water. *Phys. Chem. Chem. Phys.*, 2: 1757–1762.
40. Ma, Y.H., Pien, S., and Shelekhin, Y. (1996) Adsorption and permeation properties of vycor glass membranes. *Fundam. Adsorpt.*, 553–562.